

# Bayesian Controlled FDR Variable Selection via Knockoffs

Lorenzo Focardi-Olmi<sup>\*†</sup>, Anna Gottard<sup>‡</sup>, Michele Guindani<sup>‡</sup> and Marina Vannucci<sup>\*§</sup>

May 6, 2025

## Abstract

In many research fields, researchers aim to identify significant associations between a set of explanatory variables and a response while controlling the false discovery rate (FDR). The Knockoff filter has been recently proposed in the frequentist paradigm to introduce controlled noise in a model by cleverly constructing copies of the predictors as auxiliary variables. In this paper, we develop a fully Bayesian generalization of the classical model-X knockoff filter for normally distributed covariates. In our approach we consider a joint model of the covariates and the response variables, and incorporate the conditional independence structure of the covariates into the prior distribution of the auxiliary knockoff variables. We further incorporate the estimation of a graphical model among the covariates, leading to improved knockoffs generation and estimation of the covariate effects on the response. We use a modified spike-and-slab prior on the regression coefficients, which avoids the increase of the model dimension as typical in the classical knockoff filter. Our model performs variable selection using an upper bound on the posterior probability of non-inclusion. We show how our construction leads to valid model-X knockoffs and demonstrate that the proposed variable selection procedure leads to controlling the Bayesian FDR at an arbitrary level, in finite samples,

---

<sup>\*</sup>Department of Statistics, Rice University, USA

<sup>†</sup>Department of Statistics, Computer Science, Application "G.Parenti", University of Florence, Italy

<sup>‡</sup>Department of Biostatistics, University of California at Los Angeles, USA

<sup>§</sup>Corresponding author: marina@rice.edu

if the distribution of the covariates is fully known, and asymptotically if estimated as in the proposed model. We use simulated data to demonstrate that our proposal increases the stability of the selection with respect to classical knockoff methods, as it relies on the entire posterior distribution of the knockoff variables instead of a single sample. With respect to Bayesian variable selection methods, we show that our selection procedure achieves comparable or better performances, while maintaining control over the FDR. Finally, we show the usefulness of the proposed model with an application to real data.

**Keywords:** False Discovery Rate, Graphical Models, MCMC, Regression, Spike-and-Slab Priors.

## 1 Introduction

In recent years, variable selection has emerged as a crucial task at the forefront of statistics and machine learning, since it enables searching for associations between an outcome variable and a large amount of possible explanatory variables, when only a few of them are truly relevant. Hence, there is a need for methods that can accurately identify the subset of variables that affect the outcome. Classical approaches for variable selection typically rely on constrained optimization of the likelihood function (see, among others, Tibshirani, 1996; Fan and Li, 2001; Zou and Hastie, 2005). In the Bayesian approach, variable selection can be performed by employing several classes of prior distributions (Tadesse and Vannucci, 2021, for a review, see). For regression models, spike-and-slab priors, proposed for the first time by Mitchell and Beauchamp (1988), impose mixture distributions on the regression coefficients, with latent binary indicators that identify the relevant (active) predictors (George and McCulloch, 1997; Brown et al., 1998). Another approach involves the use of shrinkage priors to adaptively shrink coefficients towards zero (Park and Casella, 2008; Carvalho et al., 2010).

A fundamental challenge in variable selection is controlling the False Discovery Rate (FDR), to ensure the reliability and replicability of research findings. False discoveries refer to situations where a statistical procedure incorrectly identifies a variable as relevant when,

in reality, its effect is merely due to random chance or noise in the data. Several multiple testing procedures have been proposed to control the FDR - that is, the expected proportion of inactive variables mistakenly identified as active, among all those selected as active (see, for instance, Benjamini and Hochberg, 1995; Benjamini and Yekutieli, 2001, 2005). Those procedures typically rely on computing  $p$ -values, which is not always an easy task (Candès et al., 2018). Alternative methodologies have been developed by Xing et al. (2023), who propose a method that leverages a pair of mirror variables for each predictor to provide asymptotic control on the FDR, and by Dai et al. (2022), who employ a data-splitting procedure to accomplish the same goal with minimal computational effort.

In Bayesian settings, the usual definition of FDR cannot be used, since both the set of active and inactive variables are considered random. Instead, the Bayesian FDR (BFDR) is defined as an expected FDR conditionally upon the observed data, i.e., computed with respect to the posterior distribution of the sets of active/inactive variables given the observed data (Muller et al., 2006; Whittemore, 2007). An advantage of Bayesian methods is that they can facilitate multiplicity adjustments through the choice of the prior. For example, in the context of variable selection, Scott and Berger (2010) show that a spike-and-slab prior with a Beta-Bernoulli prior on the selection indicator achieves an asymptotic multiplicity control. Muller et al. (2006) and Guindani et al. (2009) prove control of the Bayesian FDR by characterizing the FDR problem as a decision problem where the optimal decision rule is based on thresholding the marginal posterior probabilities. More recently, Castillo and Roquain (2020) prove control of the Bayes FDR for general empirical Bayes multiple testing procedures. In practical settings, the optimal threshold for controlling the FDR corresponds to the minimum marginal probability of inclusion that ensures that the BFDR is less than a desired level (Newton et al., 2004). Therefore, this procedure relies on the estimates of these probabilities, which are typically obtained from the MCMC output.

Recent classical techniques to control the FDR do so by introducing carefully designed perturbations to the data. For example, Barber and Candès (2015) propose the *knock-off filter*, a powerful method that achieves finite sample FDR control in fixed-design, low-dimensional linear models. The key idea is to add controlled noise in the form of cleverly constructed copies of the predictors. These copies, called *knockoffs*, are constructed to mimic

the correlation structure of the true covariates while being statistically independent of the response. A linear model is then fitted to this augmented design, and variable selection is performed using a function of the coefficients of both the original and the knockoff variables. Essentially, knockoff variables act as negative controls. This framework has been extended to high-dimensional fixed-design settings in Barber and Candès (2019), and is often referred to as the *fixed-X knockoff* procedure. The *model-X knockoff filter* of Candès et al. (2018) further extends the approach, by avoiding assumptions on the relation between the response and the covariates. Instead, it requires full knowledge of the joint distribution of the covariates. Alternative perspectives have been investigated by Sesia et al. (2018), who provide an efficient exact sampling of the knockoff variables when the covariates are distributed as a hidden Markov model, and by Bates et al. (2021), who apply a modified version of the algorithm proposed by Candès et al. (2018) to sample knockoffs exactly in the case of known independence structure of the covariates. More recently, Berti et al. (2023) provide a new characterization of the joint distribution of the observed covariates and the knockoffs, which they define in terms of copulas. When the covariates follow a joint Gaussian distribution, their approach recovers the same solution as in Candès et al. (2018).

One of the main limitations of the classical model-X knockoff filter is that it depends on the quality of a single random draw of knockoff variables: different draws, from the same set of predictors, may yield different selected sets. To reduce this variability, Ren et al. (2023) combine the knockoff filter with the stability-selection framework of Meinshausen and Bühlmann (2010), yielding a more stable selection of active variables.

In this work, we take a fully Bayesian approach that generalizes the model-X knockoff filter and builds stability directly into the inference process. More specifically, we treat the knockoffs as latent variables and update them as part of the posterior inference. We consider the joint model of the covariates and the response, and incorporate the conditional independence structure of the covariates into the prior distribution of the knockoff variables. Our joint modeling construction employs a likelihood decomposition via auxiliary variables that allows us to obtain valid model-X knockoffs.

We further assume a Gaussian graphical model to model the covariates' dependence structure and impose a continuous spike-and-slab prior on the precision matrix (Wang, 2015).

Estimating a graphical model on the covariates allows us to obtain a coherent model that does not require perfect knowledge of the precision matrix. Moreover, unlike plug-in estimators, our Bayesian approach can naturally incorporate prior information about the conditional dependence structure of the covariates into the model. As argued by Barber et al. (2020), this leads to higher-quality knockoffs.

For the regression coefficients, we adopt the mixture spike-and-slab prior suggested by Candès et al. (2018), which avoids the increase of the model dimension typical of the classical knockoff filter. Additionally, we modify this prior by allowing the probability of inclusion of each variable to depend on the number of its neighbors in the graph. We ensure that the knockoff variables possess *a priori* the required properties outlined in Candès et al. (2018) and demonstrate that this characterization is sufficient for controlling the BFDR at an arbitrary level, in finite samples, provided the distribution of the covariates is fully known. Moreover, for a sufficiently large sample size, our procedure maintains asymptotic FDR control when the true covariates' graph is estimated from data, as in our proposed framework. In applications, to maintain control over the BFDR, we employ a greedy algorithm, similar to the one presented in Newton et al. (2004), but relying on an estimate of the upper bound for the probability of non-inclusion. Using simulated data, we show that our proposal substantially improves the stability of the selection compared to classical knockoff methods, as it leverages the entire posterior distribution of the knockoff variables rather than relying on a single realization. Furthermore, we show that our procedure achieves performance comparable to or better than standard Bayesian variable selection methods, while consistently controlling the FDR.

To our knowledge, only a few Bayesian knockoff filters have been proposed in the literature to date. Gu and Yin (2021) first considered a generalized linear model framework and assumed the distribution of the covariates to be completely known. With respect to their model formulation, in our approach, the incorporation of the estimation of a graphical model on the covariates aids in knockoff generation and improves the estimation of the covariate effects on the response. Furthermore, unlike the model formulation of Gu and Yin (2021), our joint model ensures valid model-X knockoffs. Yap and Gauran (2023) employ the Bayesian lasso of Park and Casella (2008) for the estimation of the regression coefficients. However,

they treat the covariates as fixed and require the augmented knockoff matrix to be generated prior to Bayesian inference.

The paper is organized as follows. Section 2 provides an overview of the fundamental concepts related to knockoff filters and introduces the proposed Bayesian generalization. Section 3 presents a comprehensive simulation study to evaluate the performances of the proposed method against alternative approaches. Section 4 uses an application to real data to demonstrate the practical utility of our approach. Some concluding remarks are presented in Section 5.

## 2 Methods

Let  $X = (X_1, \dots, X_p)$  be a set of covariates and  $Y$  a response variable. We observe i.i.d. data assembled in an  $(n \times p)$  data matrix  $\mathbf{X} = (x_1, \dots, x_n)$  and an  $n$ -dimensional vector  $y = (y_1, \dots, y_n)$ . In this section, we first introduce the classical notion of knockoff filters for the linear regression framework and then describe our proposed Bayesian generalization.

### 2.1 A review of the Knockoff filter

Knockoff filter is a framework that enables variable selection in an FDR-controlled environment. The main idea, originally proposed by Barber and Candès (2015), is to perturb the model by adding a set of inactive predictors built in such a way that they resemble the dependence structure of the original covariates. In Barber and Candès (2015) the knockoff predictors were built deterministically, while Candès et al. (2018) extended the framework to the model- $X$  knockoff filter, with random covariates. The model- $X$  knockoff assumes a joint distribution  $p(X)$  for the predictors and random knockoff variables,  $\tilde{X} = (\tilde{X}_1, \dots, \tilde{X}_p)$ , which are defined in a way to make it hard for the model to distinguish them from  $X$ . Formally, the knockoffs are sampled from a distribution  $p(\tilde{X} \mid X)$  such that these two properties hold:

1. Conditional Independence:

$$\tilde{X} \perp\!\!\!\perp Y \mid X$$

## 2. Pairwise Exchangeability:

$$(X, \tilde{X})_{\text{Swap}(j)} \stackrel{d}{=} (X, \tilde{X}) \quad j = 1, \dots, p,$$

where  $(X, \tilde{X})_{\text{Swap}(j)}$  results from swapping the  $j$ -th variable with the  $j$ -th knockoff. Note that while the first property is easily obtained, the second presents some difficulties (Sesia et al., 2018; Bates et al., 2021; Berti et al., 2023). A general algorithm to sample knockoffs is given in Candès et al. (2018), but it requires the computation of the conditional probability distribution of each covariate given all the others and the previously sampled knockoffs,  $p(X_j | X_{\setminus j}, \tilde{X}_{1:j-1})$ , which can be difficult to obtain for general distributions. On the other hand, when all covariates are pairwise independent, each knockoff can be sampled from the marginal distribution of  $X_j$ .

In the classical knockoff framework as proposed by Barber and Candès (2015), given the sampled knockoff variables  $\tilde{\mathbf{X}} = (\tilde{x}_1, \dots, \tilde{x}_n)$ , any model which returns a variable importance metric is fit using the augmented set of predictors  $[\mathbf{X}, \tilde{\mathbf{X}}]$ . Variable selection is performed by defining a feature statistic  $W_j$ ,  $j = 1, \dots, p$ , which combines the variable importance metric of each original predictor with the one of its own knockoff, using any antisymmetric function such that it has a symmetric distribution around zero for inactive variables. The final set of selected variables consists of those exceeding a pre-defined threshold, chosen according to a desired FDR level.

The procedure of model-X knockoffs (Candès et al., 2018) described above can be simplified if the distribution of the covariates is Gaussian. Let  $X \sim N(0, \Sigma)$ , with  $\Sigma$  the covariance matrix, then a joint distribution for which pairwise exchangeability holds is

$$(X, \tilde{X}) \sim N \left( 0, \begin{pmatrix} \Sigma & \Sigma - \text{diag}(s) \\ \Sigma - \text{diag}(s) & \Sigma \end{pmatrix} \right), \quad (1)$$

where  $s = (s_1, \dots, s_p)^T$  is a vector of values computed by minimizing the average correlation between each variable and its knockoff while ensuring that

$$\mathbf{A} = 2\text{diag}(s) - \text{diag}(s)\Sigma^{-1}\text{diag}(s) \quad (2)$$

is positive definite. Thus, by the property of the multivariate distribution, the conditional distribution of the knockoffs  $\tilde{X}$  given the covariates  $X$  is obtained as follows

$$\tilde{X} | X \sim N(X - X\Sigma^{-1}\text{diag}(s), \mathbf{A}). \quad (3)$$

Note that Equation (3) implies

$$\tilde{X} = X(I - \Sigma^{-1}\text{diag}(s)) + U. \quad (4)$$

with  $U \sim N(0, \mathbf{A})$ .

## 2.2 Constructing Bayesian knockoffs

We now introduce our Bayesian generalization of the model-X knockoff filter. We are interested in the joint model for  $Y, X$ , e.g.  $p(Y, X)$ . In particular, our interest focuses on the elements of the factorization of  $p(Y, X)$  into the conditional distribution  $p(Y|X)$  and the marginal distribution  $p(X)$ . For the latter we assume a multivariate Gaussian model as

$$X \sim N(0, \Sigma), \quad (5)$$

which implies that the joint distribution of  $(X, \tilde{X})$  is as reported in Equation (1). We then derive the conditional distribution  $p(Y | X)$  as the marginal distribution over the knockoff variables  $\tilde{X}$  of the distribution  $p(Y | X, \tilde{X})$  as

$$p(Y | X) = \int p(Y | X, \tilde{X})p(\tilde{X} | X)d\tilde{X}. \quad (6)$$

We consider a linear regression setting, where we aim at simultaneously inferring the subset of active predictors while also learning the conditional independence structure of the covariates. Thus, we specify the distribution  $p(Y | X, \tilde{X})$  as a linear regression model of the type

$$Y = X\beta + \tilde{X}\tilde{\beta} + \epsilon, \quad \epsilon \sim N(0, \sigma^2), \quad (7)$$



where  $\beta$  and  $\tilde{\beta}$  are  $p$ -dimensional vectors of the covariates' effects and the knockoffs' effects on  $Y$ , respectively. Following the decomposition introduced in Equation (4), we can rewrite the model in Equation (7) as

$$Y = X \left[ \beta + (I_p - \mathbf{\Omega} \text{diag}(s)) \tilde{\beta} \right] + U \tilde{\beta} + \epsilon, \quad \epsilon \sim N(0, \sigma^2), \quad (8)$$

where  $\mathbf{\Omega} = \mathbf{\Sigma}^{-1}$  is the precision matrix. Under this specification, it is possible to obtain the target distribution  $p(Y | X)$  in closed form as

$$p(Y | X) = \int p(Y | X, U) p(U) dU = N(X(\beta + (I_p - \mathbf{\Omega} \text{diag}(s)) \tilde{\beta}), I_n(\tilde{\beta}^T \mathbf{A} \tilde{\beta} + \sigma^2)), \quad (9)$$

with the matrix  $\mathbf{A}$  as defined in Equation (2). This construction respects the conditional independence property of the knockoff variables, as now  $Y \perp\!\!\!\perp \tilde{X} | X$ . Moreover, since the decomposition of the knockoff variables in Equation (4) is obtained from the joint distribution in Equation (1), our formulation respects the pairwise exchangeability too. Therefore, this setting uses valid model- $X$  knockoffs. Note that the construction of the Bayesian knockoff filter proposed by Gu and Yin (2021) does not produce valid knockoffs, since adopting  $p(Y | X, \tilde{X})$  as the likelihood function, as they do, implies  $Y \not\perp\!\!\!\perp \tilde{X}, X$  and therefore the conditional independence property is not satisfied.

### 2.2.1 Sparsity inducing prior for covariates' graphical model

We regard the Gaussian distribution (5) on the covariates as a graphical model and impose sparsity in the associated graph structure. Under the assumption of joint Gaussian distribution, conditional independence implies zero values in the off-diagonal elements of the precision matrix  $\mathbf{\Omega} = \mathbf{\Sigma}^{-1}$ . When  $\mathbf{\Omega}$  is sparse, also the matrix  $\mathbf{A}$  in Equation (2) is sparse, facilitating the sampling of the knockoff variables under the pairwise exchangeability property. In addition, promoting sparsity in the precision matrix  $\mathbf{\Omega}$  greatly improves computational efficiency and improves practical interpretability across various application domains. Here, we achieve this by imposing a continuous spike-and-slab prior (Wang, 2015) that combines a mixture prior distribution on the off-diagonal elements  $\omega_{jj'}$  with an exponential distribution

on the diagonal ones  $\omega_{jj}$  ( $j = 1, \dots, p$ ). Let  $\mathcal{G}$  be the undirected graph representing the conditional independences among the covariates, and let  $\mathbf{G}$  be the adjacency matrix with elements  $g_{jj'} \in \{0, 1\}$ , for  $j, j' = 1, \dots, p$  and  $j \neq j'$ , with 1 representing the presence of an edge between nodes  $(j, j')$ . Assuming the parameters in  $\mathbf{\Omega}$  independent a priori, the prior distribution can be written as

$$p(\mathbf{\Omega} \mid \mathbf{G}, v_0, v_1, \theta) = \frac{1}{K(\mathbf{G}, v_0, v_1, \theta)} \prod_{j < j'} N(\omega_{jj'} \mid 0, v_{g_{jj'}}) \prod_j \text{Exp}(\omega_{jj} \mid \theta/2), \quad (10)$$

where  $K(\mathbf{G}, v_0, v_1, \theta)$  is the normalizing constant, and where  $v_{g_{jj'}} \in \{v_0, v_1\}$ , with  $v_0$  the variance of the Gaussian distribution for the absence of an edge and  $v_1$  the variance of the edge presence. By setting a small value for  $v_0$  in the continuous spike-and-slab prior, we ensure that the entries of the precision matrix  $\mathbf{\Omega}$  corresponding to non-selected edges are close to zero. As we will see in the next section, the graphical structure is used to inform variable selection in a way that improves performances. We complete the prior by assuming independent probabilities of selecting edges as

$$p(\mathbf{G} \mid v_0, v_1, \theta, \xi) = \frac{K(\mathbf{G}, v_0, v_1, \theta)}{K(v_0, v_1, \xi)} \prod_{j < j'} \xi^{g_{jj'}} (1 - \xi)^{1 - g_{jj'}}, \quad (11)$$

where  $K(v_0, v_1, \xi)$  is the normalizing constant of the distribution and  $\xi$  is the prior probability of edge inclusion.

### 2.2.2 Priors for variable selection

For the regression coefficients, we adapt the spike-and-slab prior introduced in the supplementary material of Candès et al. (2018). Specifically, we modify their formulation by allowing each variable's inclusion probability to depend on its number of neighbors in the estimated covariate graph, as detailed below. For simplicity of exposition, here we refer to the conditional model in (7), although similar arguments apply to the marginal model (9).

We first specify the joint distribution

$$p(\beta_j, \tilde{\beta}_j \mid h_\beta, \boldsymbol{\gamma}, \sigma^2) = \begin{cases} \delta_0(\beta_j, \tilde{\beta}_j) & \text{w.p. } \mathbb{P}[\gamma_j = 0] \\ N(\beta_j \mid 0, h_\beta \sigma^2) \delta_0(\tilde{\beta}_j) & \text{w.p. } \mathbb{P}[\gamma_j = 1]/2 \\ \delta_0(\beta_j) N(\tilde{\beta}_j \mid 0, h_\beta \sigma^2) & \text{w.p. } \mathbb{P}[\gamma_j = 1]/2, \end{cases} \quad (12)$$

with  $j = 1, \dots, p$ . Here,  $h_\beta$  is a positive scaling hyperparameter and  $\boldsymbol{\gamma} = (\gamma_1, \dots, \gamma_p)^T \in \{0, 1\}^p$  is a  $p$ -dimensional vector of binary indicators such that  $\gamma_j = 1$  if  $X_j$  or its knockoff  $\tilde{X}_j$  are included in the model and, alternatively,  $\gamma_j = 0$  if neither the original feature nor the knockoff is included. By introducing two additional latent indicator vectors,  $\boldsymbol{\delta} = (\delta_1, \dots, \delta_p)$  and  $\tilde{\boldsymbol{\delta}} = (\tilde{\delta}_1, \dots, \tilde{\delta}_p)$ , such that  $\boldsymbol{\gamma} = \boldsymbol{\delta} + \tilde{\boldsymbol{\delta}}$ , the joint prior in Equation (12) can be reformulated as a mixture of independent spike-and-slab priors on  $\beta_j$  and  $\tilde{\beta}_j$  as

$$p(\beta_j, \tilde{\beta}_j \mid h_\beta, \delta_j, \tilde{\delta}_j, \sigma^2) = \delta_j N(\beta_j \mid 0, h_\beta \sigma^2) \delta_0(\tilde{\beta}_j) + \tilde{\delta}_j N(\tilde{\beta}_j \mid 0, h_\beta \sigma^2) \delta_0(\beta_j) + (1 - \delta_j - \tilde{\delta}_j) \delta_0(\beta_j, \tilde{\beta}_j).$$

Including both a covariate and its knockoff simultaneously in the model would introduce bias in the regression coefficient estimates. Therefore, we do not allow both indicators to assume value 1 and choose a multinomial distribution of the type

$$(\delta_j, \tilde{\delta}_j) \mid \gamma \sim \begin{cases} (0, 0) & \text{w.p. } \mathbb{P}[\gamma_j = 0] \\ (0, 1) & \text{w.p. } \mathbb{P}[\gamma_j = 1]/2 \\ (1, 0) & \text{w.p. } \mathbb{P}[\gamma_j = 1]/2. \end{cases}$$

Furthermore, we let the probability of success depend on the graphical model on the covariates, similar to Peterson et al. (2016), via an Ising prior of the type

$$p(\boldsymbol{\gamma} \mid \mathbf{G}, a, b) \propto \exp(a \mathbb{1}^T \boldsymbol{\gamma} + b \boldsymbol{\gamma}^T \mathbf{G} \boldsymbol{\gamma}), \quad (13)$$

where  $\mathbf{G}$  is the adjacency matrix of the undirected graph on the covariates. The hyperparameter  $a$  controls the overall sparsity of the vector  $\gamma$ , while  $b$  is linked to the graph influence on the selection. Specifically, increasing the value of  $b$  increases the probability to have  $\gamma_j = 1$  for the variables with many edges in the graph. Lastly, we complete our prior model with a conjugate prior on the variance  $\sigma^2$ ,

$$\sigma^2 \sim \text{IG}(a_\sigma, b_\sigma). \quad (14)$$

We note that Candès et al. (2018) adopt prior in Equation (12) in a fixed design Bayesian regression with augmented covariates matrix  $[\mathbf{X}, \widetilde{\mathbf{X}}]$  where  $\widetilde{\mathbf{X}}$  is sampled once from Equation (3). On the contrary, we consider the knockoffs as latent variables and update them in the posterior sampling along with the other parameters.

### 2.2.3 Markov Chain Monte Carlo for posterior sampling

Let  $\mathbf{D} = \{x_i, y_i\}_{i=1}^n$  represent the sample data and let  $\Theta$  indicate the set of unknown model parameters and latent variables,  $\Theta = \{\beta, \widetilde{\beta}, \sigma^2, \delta, \widetilde{\delta}, \gamma, \mathbf{\Omega}, \mathbf{G}\}$ . The joint posterior distribution is proportional to the product between the likelihood and the prior distributions

$$\begin{aligned} p(\Theta \mid \mathbf{D}) &\propto p(Y \mid X, \Theta) p(X \mid \Theta) p(\Theta) \propto \\ &\propto p(Y \mid X, \beta, \widetilde{\beta}, \mathbf{\Omega}, \sigma^2) p(X \mid \mathbf{\Omega}) p(\beta, \widetilde{\beta} \mid \delta, \widetilde{\delta}) p(\delta, \widetilde{\delta} \mid \gamma) p(\mathbf{\Omega} \mid \mathbf{G}) p(\gamma \mid \mathbf{G}) p(\mathbf{G}) p(\sigma^2). \end{aligned}$$

This distribution is not analytically tractable, and we therefore resort to a Markov Chain Monte Carlo (MCMC) algorithm (Brooks et al., 2011). In particular, we implement an efficient Metropolis within Gibbs scheme that employs a data augmentation (DA) scheme based on the latent variable  $U$  introduced in (4) and the formulation of the joint model detailed in Section 2.2. Specifically, as it is not possible to obtain tractable full conditional distributions using the marginal model  $p(Y \mid X, \beta, \widetilde{\beta}, \mathbf{\Omega}, \sigma^2)$ , we employ a DA step by sampling from the distribution  $p(Y \mid X, U, \beta, \widetilde{\beta}, \mathbf{\Omega}, \sigma^2)$  defined in Equation (8) and then updating  $U$  from the full conditional. We also incorporate the Add-Delete Metropolis-Hastings algorithm of Savitsky et al. (2011), that cleverly avoids having to deal with the changing dimensions of the

parameter space via a joint update of the inclusion indicators of the spike-and-slab priors and the corresponding regression coefficients. We provide full details of the MCMC algorithm in the Supplementary Material. Briefly, our algorithm is composed by the following steps:

1. We jointly update  $(\delta, \tilde{\delta}, \gamma, \beta, \tilde{\beta})$  with a stochastic search approach. At each iteration  $t = 1, \dots, T$ , we randomly select one  $j \in \{1, \dots, p\}$  and propose to change the value of  $\gamma_j$ . If the proposed  $\gamma_j^* = 0$  then the only possible choice for the proposed  $\beta_j^*, \tilde{\beta}_j^*, \delta_j^*, \tilde{\delta}_j^*$  is to set them all to 0. However, if we select a non-included variable,  $\gamma_j = 0$ , we randomly propose to include the original variable or its knockoff. More specifically, we propose the selected coefficient using a Gaussian distribution  $N(0, 0.5)$  as the proposal distribution. We then accept the proposed parameters with probability  $r = \min\{1, \rho\}$  with

$$\rho = \frac{p(Y | X, U, \beta^*, \tilde{\beta}^*, \mathbf{\Omega}, \sigma^2)p(\beta^*, \tilde{\beta}^* | \gamma^*, \sigma^2, h_\beta)p(\delta^*, \tilde{\delta}^* | \gamma^*)p(\gamma^* | \mathbf{G}, a, b)}{p(Y | X, U, \beta, \tilde{\beta}, \mathbf{\Omega}, \sigma^2)p(\beta, \tilde{\beta} | \gamma, \sigma^2, h_\beta)p(\delta, \tilde{\delta} | \gamma)p(\gamma | \mathbf{G}, a, b)}$$

To improve the mixing of the algorithm, we perform a within-model update step, proposing a new value for each selected coefficient using as proposal a distribution centered on the current value of  $(\beta, \tilde{\beta})$ .

2. We sample  $\sigma^2$  from its full conditional distribution

$$\sigma^2 | y, \mathbf{X}, U, \beta, \tilde{\beta}, \mathbf{\Omega} \sim IG[a_\sigma + \frac{n}{2}, b_\sigma + \frac{\sum_i (y_i - x_i(\beta + (I - \mathbf{\Omega} \text{diag}(s))\tilde{\beta}) - U_i\tilde{\beta})^2}{2}]$$

3. The update of  $\mathbf{G}$  and  $\mathbf{\Omega}$  is done via a block Gibbs sampler similar to the one used by Wang (2015).
4. Lastly, we update the elements of the latent auxiliary variable  $U$  from their full conditional distributions

$$u_i | y, \mathbf{X}, U, \beta, \tilde{\beta}, \mathbf{\Omega}, \sigma^2 \sim N(\mu_i, \Sigma_U)$$

$$\Sigma_U = \left( \mathbf{A} + \frac{1}{\sigma^2} \tilde{\beta} \tilde{\beta}^T \right)^{-1}$$

$$\mu_i = \Sigma_U \left( \frac{1}{\sigma^2} \left( y_i \tilde{\beta} - \tilde{\beta} \beta^T x_i - \tilde{\beta} \tilde{\beta}^T \Gamma_i \right) \right)$$

$$\Gamma = X(I - \Omega \text{diag}(s)),$$

for  $i = 1, \dots, n$ .

## 2.3 Controlling the false discovery rate

In this section, we demonstrate that our model effectively performs variable selection while controlling the Bayesian FDR. In Bayesian frameworks, the conventional definition of the false discovery rate is not directly applicable, as both the set of active and inactive variables are treated as random variables. To address this, it is customary to rely on a notion of Bayesian FDR, as discussed for example by Whittemore (2007), where it is defined as the expected value of the false discovery proportion conditioned on the observed data,  $\mathbf{D}$ , as

$$BFDR(\mathcal{S}) = \mathbb{E} \left[ \frac{|\{j \in \mathcal{S} : X_j \perp\!\!\!\perp Y\}|}{|\mathcal{S}| \vee 1} \mid \mathbf{D} \right], \quad (15)$$

where  $\mathcal{S} \subseteq \{1, \dots, p\}$  is the subset of selected indexes. Thus, the BFDR represents the expected proportion of incorrect rejections among all possible rejections, where the expectation is conditioned on the posterior distribution of active and inactive variables given the observed data. Proposition 1 states that, given an antisymmetric function  $W_j$ , our proposed method controls the BFDR at level  $q$ .

**Proposition 1.** *Let the prior distribution for the knockoff latent variable  $U$  be such that pairwise exchangeability holds, i.e.*

$$p(X, \tilde{X})_{\text{Swap}(j)} = p(X, \tilde{X}) \quad \forall j \in \{1, \dots, p\}.$$

*Let the distribution of the response variable  $Y$  follow the model in Equation (9) with prior distribution on the regression coefficient invariant to swaps, i.e.*

$$p(\beta, \tilde{\beta})_{\text{Swap}(j)} = p(\beta, \tilde{\beta}) \quad j \in \{1, \dots, p\}.$$

Then, the set  $\widehat{\mathcal{S}} = \arg \max_{\mathcal{S} \subseteq \{1, \dots, p\}} |\mathcal{S}|$  subject to

$$\frac{1}{|\mathcal{S}| \vee 1} \sum_{j \in \mathcal{S}} \{1 - \mathbb{P}[W_j > 0 \mid \mathbf{D}] + \mathbb{P}[W_j < 0 \mid \mathbf{D}]\} \leq q,$$

where  $W(\beta, \widetilde{\beta})$  is an antisymmetric function, controls the BFDR at level  $q$ .

*Proof.* Let  $r = (r_1, \dots, r_p) \in \{0, 1\}^p$  be a random vector such that  $r_j = 1 \iff X_j \perp\!\!\!\perp Y \mid X_{-j}$  with  $X_{-j} = (X_1, \dots, X_{j-1}, X_{j+1}, \dots, X_p)$ . Under a compound loss function (Muller et al., 2006), the Bayesian FDR can be written as

$$BFDR(\mathcal{S}) = \frac{\sum_{j \in \mathcal{S}} \mathbb{P}[r_j = 0 \mid \mathbf{D}]}{|\mathcal{S}| \vee 1},$$

where  $\mathbb{P}[r_j = 0 \mid \mathbf{D}]$  represents the marginal posterior probability of a covariate to be inactive. Assume for now that the random vector  $W$  satisfies the sign-flip property, i.e.

$$\mathbb{P}[W_j > 0 \mid \mathbf{D}, r_j = 0] = \mathbb{P}[W_j < 0 \mid \mathbf{D}, r_j = 0].$$

By the law of total probability, we can write

$$\begin{aligned} \mathbb{P}[W_j > 0 \mid \mathbf{D}] &= \mathbb{P}[W_j > 0 \mid \mathbf{D}, r_j = 0] \mathbb{P}[r_j = 0 \mid \mathbf{D}] \\ &\quad + \mathbb{P}[W_j > 0 \mid \mathbf{D}, r_j = 1] \mathbb{P}[r_j = 1 \mid \mathbf{D}]. \end{aligned}$$

Applying the same argument to  $\mathbb{P}[W_j < 0 \mid \mathbf{D}]$  and using the sign-flip property of  $W$ , we obtain

$$\begin{aligned} \mathbb{P}[W_j > 0 \mid \mathbf{D}] - \mathbb{P}[W_j < 0 \mid \mathbf{D}] &= \mathbb{P}[r_j = 1 \mid \mathbf{D}] \times (\mathbb{P}[W_j > 0 \mid \mathbf{D}, r_j = 1] \\ &\quad - \mathbb{P}[W_j < 0 \mid \mathbf{D}, r_j = 1]). \end{aligned}$$

Then, we can conclude,

$$\mathbb{P}[W_j > 0 \mid \mathbf{D}] - \mathbb{P}[W_j < 0 \mid \mathbf{D}] \leq \mathbb{P}[r_j = 1 \mid \mathbf{D}]. \quad (16)$$

Since  $\mathbb{P}[r_j = 0 \mid \mathbf{D}] = 1 - \mathbb{P}[r_j = 1 \mid \mathbf{D}]$ , the inequality in Equation (16) provides an upper bound for  $\mathbb{P}[r_j = 0 \mid \mathbf{D}]$ , i.e.,

$$\mathbb{P}[r_j = 0 \mid \mathbf{D}] \leq 1 - \mathbb{P}[W_j > 0 \mid \mathbf{D}] + \mathbb{P}[W_j < 0 \mid \mathbf{D}]. \quad (17)$$

To complete the proof, we need to show that an invariant prior on  $(\beta, \tilde{\beta})$  leads to a  $W$  that satisfies the sign-flip property. This result can be obtained using a similar argument as in Theorem 1 of Gu and Yin (2021). We report the proof in the Supplementary Material for completeness.  $\square$

In practice, we can compute the upper bound for  $\mathbb{P}[r_j = 0 \mid \mathbf{D}]$  in Equation (17) via Monte Carlo sampling given the MCMC output, as

$$\hat{\mathbb{P}}[r_j = 0 \mid \mathbf{D}] \leq 1 - \frac{1}{T} \left( \sum_{t=1}^T \mathbb{1}_{\{W_j^{(t)} > 0\}} - \mathbb{1}_{\{W_j^{(t)} < 0\}} \right), \quad (18)$$

where  $T$  is the number of posterior samples. A simple algorithm to construct the set  $\hat{\mathcal{S}}$  required by Proposition 1 is to compute the upper bound in Equation (18) for each covariate and sort them such that the bounds are in ascending order. Then, add variables to the set until the average of the upper bounds is below  $q$ . The final selection is not sensitive to the choice of  $W_j$ . We adopt the typical function

$$W_j = \left| \beta_j \right| - \left| \tilde{\beta}_j \right|$$

in all applications of this paper. We remark that our model performs variable selection using an upper bound on the posterior probability of non-inclusion. This strategy allows us to overcome issues with strong correlation structure among the covariates, which typically affect the state-of-art variable selection methods that rely on the estimated marginal posterior probabilities of inclusion, as empirically shown in our simulation study. Our theoretical results, indeed, show that the bound used for our variable selection procedure is not affected by the dependency structure of the covariates.

Although Proposition 1 shows that our method controls the BFDR at a threshold  $q$ , it



assumes that the latent variables  $\tilde{X}$  are valid knockoffs a priori. As discussed by Candès et al. (2018), the construction of valid model-X knockoffs requires perfect knowledge of the covariates' distribution. However, our proposed model assumes that the covariates  $X$  follow a Gaussian distribution, with an unknown precision matrix that must be estimated from the data. Barber et al. (2020) prove that the knockoff procedure maintains FDR control at a desired threshold  $q$  if the precision matrix of the Gaussian model is correctly estimated. Here, we show that, under mild regularity conditions, the priors chosen to estimate the Gaussian graphical model for the covariates yield accurate posterior estimates of the precision matrix. Thus, drawing on similar arguments as in Barber et al. (2020), we can conclude that our procedure controls both the frequentist FDR and, consequently, the expected BFDR (Guindani et al., 2009) in large samples, even if the precision matrix is unknown. More precisely, we are able to prove that the posterior convergence rate of our estimator is the same as the one of the Bayesian graphical lasso. To show such result, we first need to prove that our prior distribution assigns enough probability mass to values “close” to the true one.

**Proposition 2.** *Let the true precision matrix  $\mathbf{\Omega}_0 \in \mathcal{U}(\epsilon_0, l) = \{\mathbf{\Omega} : |\{(i, j) : 1 \leq i < j \leq p, \omega_{ij} \neq 0\}| \leq l, 0 < \epsilon_0 \leq \text{eig}(\mathbf{\Omega})_1 < \text{eig}(\mathbf{\Omega})_p \leq \epsilon_0^{-1} < \infty\}$  for some  $0 < \epsilon_0 < \infty$  and  $0 \leq l \leq p(1 - p)/2$ . Also assume that the prior distributions for the precision matrix  $\mathbf{\Omega}$  and the adjacency matrix  $\mathbf{G}$  are:*

$$p(\mathbf{\Omega} \mid \mathbf{G}, v_0, v_1, \theta) = \frac{1}{K(\mathbf{G}, v_0, v_1, \theta)} \prod_{j < j'} N(\omega_{jj'} \mid 0, v_{g_{jj'}}) \prod_j \text{Exp}(\omega_{jj} \mid \theta/2)$$

with  $v_{g_{ij}} \leq \frac{\|\mathbf{\Omega}_0\|_\infty}{2 \log 2}$  and

$$p(\mathbf{G} \mid v_0, v_1, \theta, \xi) = \frac{K(\mathbf{G}, v_0, v_1, \theta)}{K(v_0, v_1, \xi)} \prod_{j < j'} \xi^{g_{jj'}} (1 - \xi)^{1 - g_{jj'}},$$

with  $\xi < 0.5$ . Then,

$$\Pi(B(p_{\Omega_0}, \epsilon_n)) \gtrsim (c\epsilon_n/p)^{p+l},$$

with  $\Pi(\cdot)$  the probability under the prior distribution,  $B(p_{\Omega_0}, \epsilon_n) = \{p : K(p_{\Omega_0}, p_{\Omega}) \leq \epsilon_n^2, V(p_{\Omega_0}, p_{\Omega}) \leq \epsilon_n^2\}$  with  $K(f, g) = \int f \log(f/g)$  and  $V(f, g) = \int f \log^2(f/g)$  and  $p_{\Omega_0}$  and

$p_{\Omega}$  the density functions of  $N(0, \mathbf{\Omega}_0)$  and  $N(0, \mathbf{\Omega})$  respectively.

*Proof.* See the Supplementary Material.  $\square$

Using the prior concentration result stated in Proposition 2, we can investigate the posterior convergence rate of the graphical parameters. Proposition 3 shows how the posterior convergence rate of our model is equal to the convergence rate of the graphical lasso (Friedman et al., 2008) and the Bayesian graphical lasso (Park and Casella, 2008). Note that, in Proposition 3, the prior distribution for the precision matrix in Equation (19) is slightly different from the one used in our model in Equation (11) since it includes the probability  $\mathbb{P}[\bar{R} \geq |\mathbf{G}|]$  to penalize denser graphs. However, in the context of MCMC algorithm to sample from posterior distribution, such probability has little to no effect. The ratio of these probabilities is, indeed, close or superior to 1 for most proposal distributions.

**Proposition 3.** *Let  $X^{(n)} = (X_1, \dots, X_n)$  be a random sample from the  $p$ -dimensional Gaussian distribution with mean 0 and precision matrix  $\mathbf{\Omega}_0 \in \mathcal{U}(\epsilon_0, l) = \{\mathbf{\Omega} : |\{(i, j) : 1 \leq i < j \leq p, \omega_{ij} \neq 0\}| \leq l, 0 < \epsilon_0 \leq \text{eig}(\mathbf{\Omega})_1 < \text{eig}(\mathbf{\Omega})_p \leq \epsilon_0^{-1} < \infty\}$  for some  $0 < \epsilon_0 < \infty$  and  $0 \leq l \leq p(1 - p)/2$ . Also assume that the prior distributions are:*

$$p(\mathbf{\Omega} \mid \mathbf{G}, v_0, v_1, \theta) = \frac{1}{K(\mathbf{G}, v_0, v_1, \theta)} \prod_{j < j'} N(\omega_{jj'} \mid 0, v_{g_{jj'}}) \prod_j \text{Exp}(\omega_{jj} \mid \theta/2)$$

with  $v_{g_{ij}} \leq \frac{\|\mathbf{\Omega}_0\|_{\infty}}{2 \log 2}$  and

$$p(\mathbf{G} \mid v_0, v_1, \theta, \xi) = \frac{K(\mathbf{G}, v_0, v_1, \theta)}{K(v_0, v_1, \xi)} \prod_{j < j'} \xi^{g_{jj'}} (1 - \xi)^{1 - g_{jj'}} \mathbb{P}(\bar{R} \geq |\mathbf{G}|), \quad (19)$$

with  $\xi < 0.5$  and  $\mathbb{P}(\bar{R} > a_1 m) \leq \exp\{-a_2 m \log m\}$  for some constants  $a_1$  and  $a_2$  and  $m = 1, 2, \dots$ . Then,

$$\mathbb{E}_0[\mathbb{P}\{\|\mathbf{\Omega} - \mathbf{\Omega}_0\|_2 > M\epsilon_n \mid X^{(n)}\}] \rightarrow 0$$

for  $\epsilon_n = n^{-1/2}(p + l)^{1/2}(\log p)^{1/2}$  and sufficiently large constant  $M$ .

*Proof.* See the Supplementary Material.  $\square$

Proposition 3 shows that, with sufficiently small prior variances, the posterior mean of the precision matrix  $\mathbf{\Omega}$  converges to the true one with the same rate as the convergence rate of graphical lasso (Rothman et al., 2008). Therefore, employing similar arguments as in Barber et al. (2020), for a sufficiently large sample size, our model controls the frequentist FDR and, consequently, the expected BFDR under a threshold  $q$  without the knowledge of the true precision matrix  $\mathbf{\Omega}$ .

### 3 Simulation study

We evaluate the performance of the proposed model through a comprehensive simulation study and compare results with those of the classical model-X knockoff filter and state-of-the-art variable selection methods, including lasso regression (Tibshirani, 1996) and models that use discrete spike-and-slab priors (Mitchell and Beauchamp, 1988).

#### 3.1 Data generation

We generated data from a few distinct scenarios. In Scenario 1, we generated  $p = 30$  covariates independently sampled from a standard Gaussian distribution. Out of the 30 covariates, we assumed that 6 of them have a linear effect on the response variable  $y$ . The regression coefficients associated with these active covariates were randomly selected from the set  $\{\pm 0.5, \pm 1, \pm 1.5\}$  to introduce variation in the strength of the effects. We then simulated the response variable from the linear equation  $y_i = x_i\beta + \epsilon_i$ , with  $\epsilon_i \sim N(0, \sigma_\epsilon)$  and  $\sigma_\epsilon = 1$ , for  $i = 1, \dots, n$ . This relatively simple scenario enables us to assess the capability of our model to recover the set of active variables when the graphical structure learning is, effectively, a source of noise in the model. In Scenario 2, we introduce a more realistic setting by incorporating a correlation structure among the predictors. More specifically, the 30 covariates were generated from a Gaussian graphical model, where the underlying graph structure is characterized by a sparse precision matrix. The underlying graph structure is shown in Figure 1. Similarly to Scenario 1, we selected 6 out of the 30 variables to be active in explaining the response  $y$  and randomly sampled their coefficient values from the set  $\{\pm 0.5, \pm 1\}$ . In Scenario 3, data are simulated following the setting of Li and Li (2008)

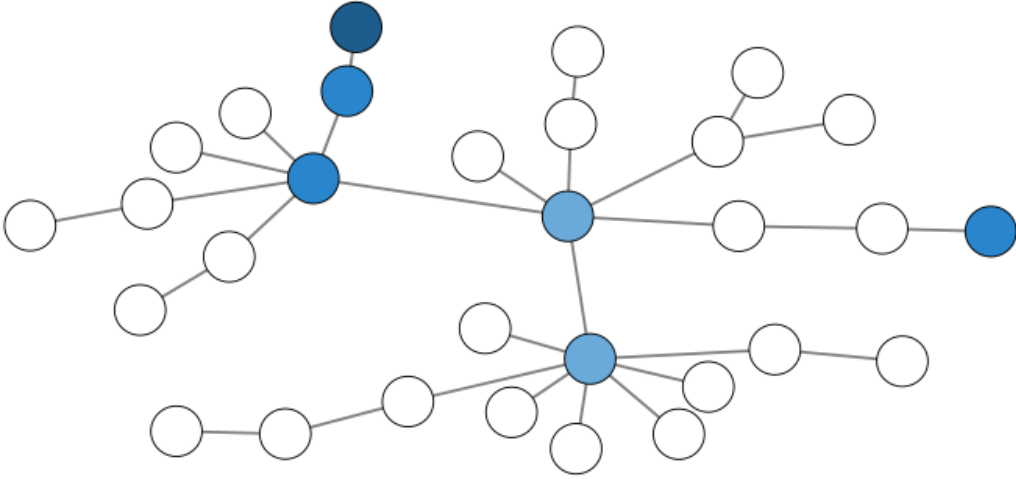


Figure 1: **Simulation study:** Scale-free graph structure under Gaussian graphical model in Scenario 2. White nodes correspond to the noise variables, and blue nodes to the active ones. A stronger blue color corresponds to a larger effect.

and Peterson et al. (2016). Specifically, we generated the covariates from a graph with 40 hubs, each with 5 connected nodes. This resulted in 240 covariates with a sparse graphical model of 200 edges in total. We set as active variables those in the first 4 hubs, plus their connected edges, resulting in a total of 24 non-zero coefficients. In particular the regression coefficients of the 4 hubs are 5,  $-5$ , 3 and  $-3$ , respectively, while the coefficients of the associated nodes are the same but divided by  $\sqrt{10}$ . The covariates were then generated from a Gaussian distribution with zero mean and covariance matrix  $\Sigma$  with diagonal elements equal to 1 and covariances between connected variables equal to 0.7. As in the previous scenarios, the response variable was simulated from a linear Gaussian model with the error variance equal to  $\sum_j \beta_j^2/4$ . In each scenario we set the sample size at  $n = 200$  and considered 100 replicated data sets.

### 3.2 Parameter settings

When fitting our model, we need to specify the hyperparameters of the shrinkage inducing prior (10) on the precision matrix of the covariates' graph, the spike-and-slab priors (12) on the regression coefficients and the Ising prior (13) on the selection indicators. In all analyses, for prior (10) on the precision matrix, following the recommendations in Wang (2015), we

used  $v_0 = 0.01^2$  and  $v_1 = hv_0$  with  $h = 100$ . We set the prior probability of edge selection  $\xi$  to 0.01 and the exponential parameter  $\theta$  for the elements on the diagonal to 2. To specify vaguely informative priors, we set  $h_\beta = 1$  in the joint prior (12) on the regression coefficients, and  $\alpha_\sigma = \beta_\sigma = 2$  for the prior (14) on the error variance. Furthermore, we centered covariates and response variables, ensuring that the intercept term in the model is zero. Smith (1973) showed that, in the Bayesian framework, setting the intercept term to zero is equivalent to placing a Gaussian prior with infinite variance on the intercept parameter. Finally, for the Ising prior (13) on  $\gamma$ , we set  $a = b = 0.5$ . This specification corresponds to a prior inclusion probability of 0.622 on the original variable or its knockoff, when the graph is empty. When experimenting with this prior, we found non-sparse specifications to work well, as the Bayesian knockoff framework allows for further control of the FDR by excluding inactive covariates. We provide sensitivity analyses to these prior choices in Section 3.5.

When initializing the MCMC algorithm, we set the selection indicators  $\gamma$  to 0 and assumed independent covariates with  $\boldsymbol{\Omega} = \mathbf{I}$ . The results reported below in Section 3.3 are obtained by running MCMC chains with 8,000 iterations for burn-in, followed by 8,000 iterations for inference. For each chain, we assessed convergence by using the Geweke’s diagnostic test (Geweke, 1992) to check for signs of non-convergence. For example, the average  $z$ -scores from the test for  $\{(\beta_j, \tilde{\beta}_j)\}_{j=1}^p$  were 0.03, 0.01 and  $-0.05$  for Scenario 1, Scenario 2 and Scenario 3, respectively. This suggests that the algorithm has run for enough iterations.

### 3.3 Results and comparisons

Let us first examine a single data set to gain insight into how the proposed model works. Specifically, we focus on a randomly selected data set generated under Scenario 3. The top plot of Figure 2 shows the estimated BFDR and the upper bound for  $\mathbb{P}[r_j = 0 \mid \mathbf{D}]$ , for  $j = 1, \dots, p$  and covariates sorted by the BFDR values. Our method correctly identifies 18 of the 24 true predictors with 6 false negatives, for a  $q = 0.1$  threshold on the BFDR. The bottom plot of Figure 2 reports the PPIs of all covariates, calculated by fitting a traditional Bayesian linear regression model with discrete spike-and-slab priors and a Beta hyperprior on the inclusion probability of the latent indicators (George and McCulloch, 1997; Brown et al., 1998; Vannucci, 2021). This method selects 21 of the 24 true predictors with 44 false

positives, for a 0.5 threshold on the PPIs. The large number of false positives is due to the fact that the presence of collinearity in the data greatly affects the PPIs values, resulting in inflated values for inactive covariates that are correlated to the active ones. This simple example highlights the inability of clearly dividing active and inactive variables based on the posterior probability values. The results are confirmed in the comparison study below, that shows performance values averaged over replicated datasets. This empirical comparison of our Bayesian Knockoff with a traditional spike and slab regression confirms the theoretical results in Theorem 1, where the upper bound is unaffected by the covariates' dependency structure.

Next, we report results of our method averaged over 100 replicated datasets and perform a comparison of the performances with other procedures for variable selection, with and without FDR control. Among these procedures, we include the classical model-X knockoff filter proposed by Barber and Candès (2019). In particular, we consider two versions of the model-X knockoff filter, one with the true covariance matrix assumed known, and one with an estimate of  $\Sigma$  obtained via the graphical lasso estimator of Friedman et al. (2008). Indeed, Barber et al. (2020) proved that, under certain conditions, the graphical lasso can be used to preserve the FDR guarantees of knockoff filters. For both our model and the classical knockoff filter, we fix the FDR threshold at  $q = 0.1$ . The knockoffs were generated using the R package `knockoffs`, and the covariance matrix was estimated using the `glasso` package. In addition to the model-X knockoff filter, our comparison includes other state-of-art methods for variable selection. In particular, we include the Lasso regression (Tibshirani, 1996) and a Bayesian linear regression model with discrete spike-and-slab prior and a Beta hyperprior on the inclusion probability, which we implemented ourselves. We also considered the joint edge and regression estimation model proposed by Peterson et al. (2016), which we implemented ourselves as a version of our proposed model without knockoffs latent variables. The regularizing parameter for lasso regression was determined by minimizing the cross-validated error using the R package `glmnet`. We note that this method does not employ any FDR correction. Variable selection for the Bayesian and joint estimation methods was achieved by thresholding the marginal posterior probabilities of inclusion (PPIs) at 0.5, following the median model approach (Barbieri and Berger, 2004). We also considered the

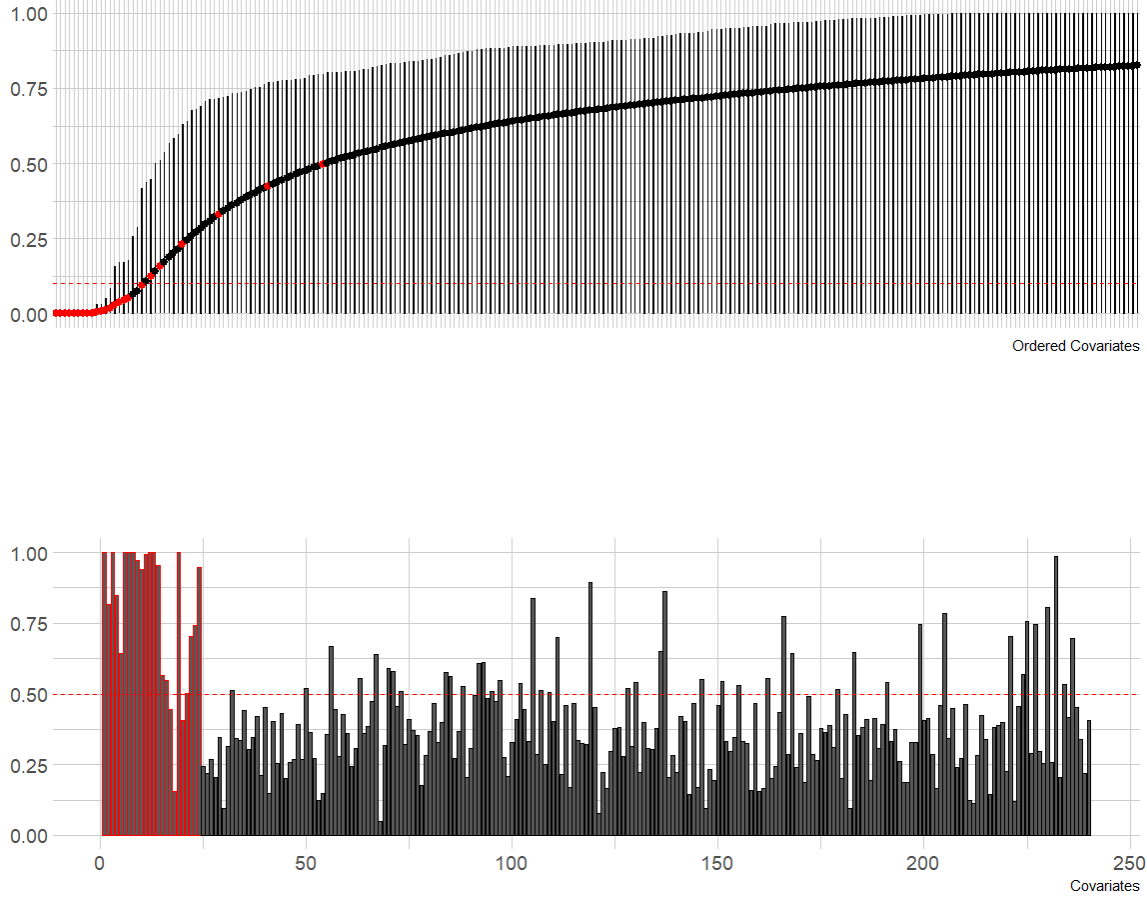


Figure 2: **Simulation study:** Variable selection performed by our Bayesian knockoff filter method (BayeKnock) and by spike-and-regression (Spike-Slab) on a simulated dataset under Scenario 3. *Top plot (BayesKnock):* Bars represent estimates of the upper bound for  $\mathbb{P}[r_j = 0 | D]$  as in Equation (17) while points represent the estimated BFDR. Red points correspond to true active variables. *Bottom plot (Spike-Slab):* Estimated marginal posterior probabilities of inclusion (PPIs). Red bars correspond to true active variables.

BFDR approach proposed by Newton et al. (2004).

To compare performance, in Table 1 we report averages and standard deviations across 100 replicates of several evaluation metrics. In particular, we consider FDR, True Positive Rate (TPR), Matthew Correlation Coefficient (MCC), and F1-score. Let TP be the number of true positives, TN the number of true negatives, FP the number of false positives, and FN the number of false negatives. We can then define the performance metrics used as

$$\begin{aligned} FDR &= \frac{FP}{FP + TP}, & TPR &= \frac{TP}{TP + FN}, \\ MCC &= \frac{TP \times TN - FP \times FN}{\sqrt{(TP + FP)(TP + FN)(TN + FP)(TN + FN)}}, \\ F1 &= \frac{2 \times TP}{2 \times TP + FP + FN}. \end{aligned}$$

Results in Table 1 indicate that the proposed Bayesian method succeeds in keeping the FDR below the given threshold in every scenario, while achieving strong performances in TPR compared to the other methods, as well as MCC and F1 scores. It is worth noting that the classical knockoff filter exhibits low TPR in Scenarios 1 and 2, where the magnitude of the true coefficients is rather small. In other settings, not reported here, where the signal was strong and the sample size larger, we noticed improved performances for all methods, including classical knockoffs. Further, the values of the standard deviations for the TPR of the knockoff filter in the first two scenarios are higher than those of the other methods. This happens because, across the 100 simulated data sets, the knockoff filter TPR is often zero and sometimes quite high. Finally, we note that classical knockoff has a slightly higher FDR than the threshold 0.1 when the covariates are not independent and the covariance matrix is estimated using graphical lasso. As shown in Barber et al. (2020), the classical knockoff filter does not control FDR exactly below  $q$  when the covariance matrix used to build the knockoffs is not the true one but an estimate. In our case, the graphical lasso tends to produce a sparser than needed graph. This behavior also supports our choice of setting the parameter of the priors in the proposed method to obtain a generally dense graph to be used to generate the knockoffs. Results for the third scenario confirm that the proposed Bayesian Knockoff filter is also able to outperform the state-of-art methods in settings with



larger dimensionality. As a matter of fact, it successfully controls FDR under 0.1, unlike the lasso regression. Moreover, the TPR is on average comparable to the one of the classical knockoff filter, but it is more stable as it has a much lower standard deviation.

As for the comparison with the state-of-art methods for variable selection, we can see that Lasso has a high TPR in every scenario but also a high FDR. Indeed, Meinshausen and Bühlmann (2006) noted that the lasso estimator tends to include too many inactive predictors when the penalization parameter is chosen to have low prediction error, as we did in our simulations. Compared with Bayesian variable selection via spike-and-slab prior, our model offers comparable results in the first two scenarios, where the covariates are independent, with almost perfect results. In the third scenario, with dependent covariates, spike-and-slab loses the control of FDR, unlike our method, even though it manages to find more relevant predictors than our method. In Table 1 we do not show results for the BFDR approach proposed by Newton et al. (2004). Indeed, BFDR selected exactly the same variables as spike-and-slab in the first two scenarios. In the third scenario, however, the PPIs were hovering around 0.5 and the BFDR did not select any variable. As pointed out in the introduction section, Bayes FDR selection procedures rely on the estimates of the marginal PPIs, as obtained from the MCMC output, while our procedure employs an upper bound on the probabilities of non-inclusion. Therefore, our model appears to achieve good operating characteristics and to control the FDR even when the estimates of the marginal posterior probability of inclusion fail to select the true relevant variables. This is evident when comparing our method with the model proposed by Peterson et al. (2016) (Joint). In scenarios 1 and 2 the two methods have the same performances, while in scenario 3, even though MCC and F1 have similar values, the addition of the knockoffs allows to keep the FDR under the desired level, while the joint method has higher FDR and therefore not an explicit control over it.

We note that, with our proposed method, posterior inference results not only in variable selection but also in learning the underlying graph structure among the covariates via the inference on the precision matrix  $\mathbf{\Omega}$ . For example, the median graph can be obtained by thresholding the marginal posterior probability of inclusion (PPI) of edge inclusion at 0.5. This approach of using a threshold for PPIs is commonly employed in graph structural

Table 1: **Simulation study:** FDR, TPR, MCC and F1-score, for the scenarios described in Section 3.1. Compared methods are the proposed model (BayesKnock) classical Knockoff filter with exact (Knockoff (Exact)) and estimated (Knockoff (Glasso)) covariance matrix, Lasso, spike-and-slab regression (Spike-Slab) and the joint model proposed by Peterson et al. (2016) (Joint). Values reported are averages over 100 replicated data sets, with standard deviations in parentheses.

		Scenario 1		Scenario 2		Scenario 3	
FDR	BayesKnock	<b>0.007</b>	(0.03)	<b>0.013</b>	(0.05)	<b>0.032</b>	(0.05)
	Knockoff (Exact)	0.035	(0.11)	0.025	(0.09)	<b>0.055</b>	(0.08)
	Knockoff (Glasso)	0.070	(0.16)	0.114	(0.19)	0.079	(0.08)
	Lasso	0.543	(0.14)	0.557	(0.12)	0.437	(0.12)
	Spike-Slab	<b>0.000</b>	(0.00)	<b>0.003</b>	(0.02)	0.716	(0.04)
	Joint	0.029	(0.06)	0.043	(0.07)	0.177	(0.11)
TPR	BayesKnock	<b>1.000</b>	(0.00)	0.977	(0.07)	0.560	(0.10)
	Knockoff (Exact)	0.088	(0.28)	0.068	(0.25)	0.592	(0.36)
	Knockoff (Glasso)	0.162	(0.37)	0.277	(0.45)	0.595	(0.39)
	Lasso	<b>1.000</b>	(0.00)	<b>1.000</b>	(0.00)	<b>0.934</b>	(0.05)
	Spike-Slab	0.999	(0.01)	0.979	(0.06)	<b>0.820</b>	(0.06)
	Joint	<b>1.000</b>	(0.00)	<b>1.000</b>	(0.00)	0.664	(0.08)
MCC	BayesKnock	<b>0.995</b>	(0.02)	<b>0.973</b>	(0.06)	<b>0.714</b>	(0.07)
	Knockoff (Exact)	0.065	(0.21)	0.059	(0.20)	0.627	(0.37)
	Knockoff (Glasso)	0.109	(0.25)	0.188	(0.31)	0.612	(0.41)
	Lasso	0.544	(0.15)	0.536	(0.14)	0.682	(0.09)
	Spike-Slab	<b>0.999</b>	(0.01)	<b>0.986</b>	(0.05)	0.389	(0.05)
	Joint	0.981	(0.04)	0.972	(0.05)	<b>0.711</b>	(0.08)
F1	BayesKnock	<b>0.996</b>	(0.02)	<b>0.977</b>	(0.06)	<b>0.704</b>	(0.08)
	Knockoff (Exact)	0.069	(0.22)	0.062	(0.21)	0.631	(0.37)
	Knockoff (Glasso)	0.117	(0.27)	0.201	(0.33)	0.629	(0.38)
	Lasso	0.614	(0.12)	0.608	(0.11)	0.693	(0.09)
	Spike-Slab	<b>0.999</b>	(0.01)	0.988	(0.04)	0.420	(0.04)
	Joint	0.985	(0.03)	<b>0.977</b>	(0.04)	<b>0.729</b>	(0.07)

learning tasks as the space of possible graphs is too big to be explored entirely, making it impossible to select the most frequently encountered graph. When looking at the Frobenius norm of the difference between the posterior mean of  $\mathbf{\Omega}$  and the true precision matrix,

$$\|\mathbf{\Omega} - \hat{\mathbf{\Omega}}\|_F = \sqrt{\sum_{i,j} (\omega_{ij} - \hat{\omega}_{ij})^2},$$

our model achieved very solid performances for graph selection across the scenarios. For example, the average Frobenius norm was 1.404, 1.415 and 9.425 and the F1-score was 0.869, 0.865 and 0.99 in Scenarios 1, 2 and 3, respectively. Note that the Frobenius norm is much higher in Scenario 3 due to the different magnitude in the correlation between variables. However, as we can see from the F1-score, the graph recovery still works.

### 3.4 Simulation of a survival outcome from an accelerated failure time model

We also show a simulation for a regression model with a survival outcome, specifically an accelerated failure time (AFT) model, with censored observations. To use the proposed Bayesian knockoff filter, we adapt the stochastic search MCMC procedure of Sha et al. (2006), that makes use of data augmentation techniques (Tanner and Wong, 1987). Let  $T_i$  represent the time-to-event for the  $i$ -th subject and  $c_i$  the censoring time. AFT models assume a multiplicative effect on the survival times of the general form  $\log(T_i) = X_i\beta + \epsilon_i$ , where the errors  $\epsilon_i$  may have several distributions. Here, we assume the errors to be i.i.d. Gaussian variables. To allow for censored observations, we introduce a latent variable  $y_i$  such that

$$\begin{cases} y_i = \log(T_i^*) & \text{if } \kappa_i = 1 \\ y_i > \log(T_i^*) & \text{if } \kappa_i = 0 \end{cases}.$$

where  $T_i^*$  is defined as  $\min(T_i, c_i)$  and  $\kappa_i = \mathbb{1}_{T_i \leq c_i}$  is the censoring indicator. Here, we assume that the latent variable  $y_i$  given the covariates  $X$  follows the model described in Equation (9) with  $p(Y | X, U)$  as in Equation (8), with the same prior specification. We generate the covariates following the scheme employed in Scenario 3 above, and then generate

Table 2: **Simulation study:** FDR, TPR, MCC and F1-score, for the AFT models. Compared methods are the proposed model (BayesKnock), spike-and-slab regression (Spike-Slab) and the joint model proposed by Peterson et al. (2016) (Joint). Values reported are averages over 100 replicated data sets, with standard deviations in parentheses.

	FDR		TPR		MCC		F1	
BayesKnock	<b>0.035</b>	(0.03)	0.526	(0.11)	<b>0.713</b>	(0.08)	0.701	(0.10)
Spike-Slab	0.642	(0.04)	<b>0.742</b>	(0.01)	0.239	(0.08)	0.311	(0.08)
Joint	0.192	(0.13)	0.592	(0.04)	0.701	(0.09)	<b>0.712</b>	(0.10)

the log of the survival times from the linear AFT model. We allow for 25 % of the subjects to be censored. Table 2 shows performances of our proposed method, compared to the spike-and-slab method for AFT models of Sha et al. (2004) and to the same AFT model without knockoff latent variable, as also implemented by Peterson et al. (2016). These results are consistent with those for Scenario 3 in the previous simulation and also show that the proposed procedure suffers the least from the presence of censored data.

### 3.5 Sensitivity analysis

Table 3 shows the results of the sensitivity analysis. We started from the same setting adopted in the simulation study for Scenario 2 and then varied one hyperparameter at a time. We found that posterior inference is robust to the choice of the hyperparameters, except for  $v_0$  in the prior on the precision matrix  $\mathbf{\Omega}$  in Equation (10). Both Wang (2015) and Peterson et al. (2016) report the same sensitivity. We notice, however, that the choice of  $v_0$  does not affect the selection performances of our method. As noted in Barber et al. (2020), knockoffs can still be used with estimated distributions, but the control on FDR is affected by the Kullback-Leiber distance between the estimate and the true distribution. As a matter of fact, in Gaussian graphical models, imposing too many zeros strongly affects the estimates of the non-zero off-diagonal elements on the precision matrix  $\mathbf{\Omega}$ . For this reason, we recommend setting the hyperparameters  $v_0$  and  $v_1$  to obtain a slightly denser graph.

Table 3: **Simulation study:** Sensitivity analysis.

Hyperparameter	FDR	TPR	Frobenius Loss	F1 Score
$a = -2.5$	0.000	1.000	1.624	0.800
$a = -0.5$	0.000	1.000	1.617	0.840
$a = 0.5$	0.000	1.000	1.607	0.824
$a = 2.5$	0.142	1.000	1.662	0.800
$b = -2.5$	0.000	0.833	1.625	0.816
$b = -0.5$	0.000	0.833	1.600	0.840
$b = 0.5$	0.000	1.000	1.607	0.824
$b = 2.5$	0.333	1.000	1.645	0.816
$v_0 = 0.01^2$	0.000	1.000	1.620	0.816
$v_0 = 0.1^2$	0.000	1.000	2.435	0.067
$v_0 = 0.5^2$	0.000	1.000	4.134	0.000
$v_1 = 0.25$	0.000	1.000	1.525	0.840
$v_1 = 1.00$	0.000	1.000	1.645	0.816
$v_1 = 25.00$	0.000	1.000	1.708	0.840
$v_1 = 100.00$	0.000	1.000	1.901	0.766

## 4 Application to prostate cancer data

As an illustrative example, we examine a data set on prostate cancer obtained from Stamey et al. (1989) and widely used as a benchmark data set (see, for instance, Tibshirani, 1996; Zou and Hastie, 2005, among others). The aim is to investigate the association between Prostate-Specific Antigen (PSA) levels and various clinical measures in a sample of 97 men, who were preparing to undergo radical prostatectomy. PSA is a protein produced by normal and malignant prostate cells and is useful as a preoperative marker as prostate cancer releases PSA into the bloodstream. Additionally, eight clinical measures are included: the logarithm of the cancer volume (in  $\text{cm}^3$ ) (`lcavol`), the logarithm of the prostate weight (in g) (`lweight`), patient age (`age`), the logarithm of the bad prostatic hyperplasia (in  $\text{cm}^2$ ) (`lbph`), the logarithm of capsular penetration (in cm) (`lcp`), seminal vesicle invasion (`svi`), the current Gleason score (`gleason`) and the percentage of Gleason scores four or five out of five (`pgg45`). The logarithm of the PSA (ng/ml) is the response variable. The presence of seminal vesicle invasion is a binary variable (1 = yes, 0 = no) and `gleason` is a discrete numerical variable with four values. The Gleason score relates to the current grade of prostate cancer, while the predictor `pgg45` provides information about the patient’s history of the

Gleason scores, and it is strongly linked to the current final score Gleason score.

For our analysis, we considered the subset of 73 subjects without seminal vesicle invasion and with no severe cancer (Gleason score less than 9). To ensure the appropriate statistical assumptions, we applied the nonparanormal transformation (Liu et al., 2009) to the covariates. This transformation provides a Gaussian marginal distribution of each covariate and assumes a Gaussian copula on their joint distribution. We tested the joint Gaussian assumption after this transformation using the multivariate Shapiro test (Villasenor Alva and Estrada, 2009), obtaining a  $p$ -value of 0.02. In our application, we used the same hyperparameter settings as in the simulation study, and ran an MCMC chain with 8,000 iteration for burn-in followed by 8,000 iterations for inference. The average  $z$ -scores from the Geweke’s test for  $\{(\beta_j, \tilde{\beta}_j)\}_{j=1}^p$  was  $-0.22$ .

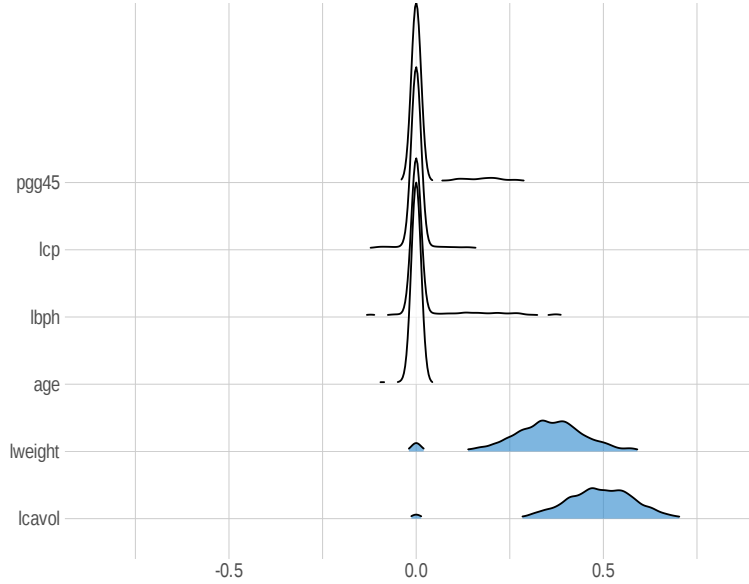


Figure 3: **Prostate cancer data:** Posterior distribution of  $W_j$ ,  $j = 1, \dots, 6$ . Those highlighted in blue are selected according to Figure 4

Figure 3 shows the posterior distribution of the feature statistics  $W_j$ ,  $j = 1, \dots, p$  for each covariate in the model, with the selected variables shown in blue. Notably, the posterior distribution of the non-selected variables is symmetric around zero, while the selected variables exhibit a positive-centered distribution. Additionally, Figure 4 reports the estimated values of  $2\hat{\mathbb{P}}[W_j \leq 0 \mid \mathbf{D}]$ ,  $j = 1, \dots, 6$ , in increasing order, together with the corresponding estimated  $\text{BFDR}(\mathcal{S})$ . Therefore, setting  $q = 0.1$ , the covariates to be selected are the logarithm

Table 4: **Prostate cancer data:** Selection of variables using different variable selection methods.

Variable	BayesKnock	Knockoff Filter	Lasso	Spike-and-slab	Joint
lcavol	✓	-	✓	✓	✓
lweight	✓	-	✓	✓	✓
age	-	-	-	-	-
lbph	-	-	✓	-	✓
lcp	-	-	-	-	-
pgg45	-	-	✓	-	-

of cancer volume and the logarithm of prostate weight.

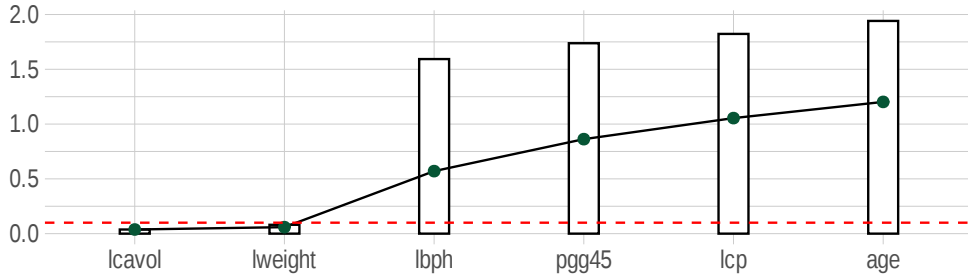


Figure 4: **Prostate cancer data:** Variable selection. Bars represent estimates  $2\hat{\mathbb{P}}[W_j \leq 0 | \mathbf{D}]$ ,  $j = 1, \dots, 6$ , in increasing order and points represent the estimated  $\text{BFDR}(\mathcal{S})$  with  $\mathcal{S}$  the set of all previous indexes. The dashed red line is the chosen threshold  $q = 0.1$ .

We also applied the state-of-art procedures used for comparison in the simulation study. Table 4 summarizes the results. We can see that classical knockoff filter does not find any association between covariates and PSA production level. Spike-and-slab regression selects the same covariates as the proposed method, and the joint estimation model selects one additional variable. Lasso, as we saw in the simulation study, selects many variables, including the two selected by our method. We acknowledge that the Bayesian procedures are computationally more expensive than the classical methods. For example, running the MCMC for our proposed method on this application took 35 minutes on a regular laptop equipped with Intel(R) Core(TM) i7-9750H CPU @ 2.60GHz. However, relying on a posterior distribution of the knockoff variables increases stability of the selection, as our simulations have shown.

## 5 Concluding remarks

In this article, we have proposed a fully Bayesian generalization of the model-X knockoff filter of Candès et al. (2018) that allows for variable selection while controlling the BFDR at an arbitrary level. Our framework treats knockoff variables as latent variables that act as negative controls. Additionally, we have imposed a sparse conditional independence structure on the covariates and used it in the prior on the knockoffs in a way that satisfies their pairwise conditional independence property. We have also limited the computational cost by adopting a modified version of the spike-and-slab prior that avoids the increase of the model dimension. Our model performs variable selection using an upper bound on the posterior probability of non-inclusion. We have shown how our model construction leads to valid model-X knockoffs and demonstrated that the proposed approach is sufficient for controlling the BFDR at an arbitrary level, in finite samples, if the distribution of the covariates is fully known, and asymptotically if estimated as in our model.

In applications, we have shown that our proposal increases the stability of the selection, since it relies on the entire posterior distribution of the knockoff variables instead of a single sample. Results from our simulation study have shown how in simple settings (like Scenarios 1 and 2) our Bayesian knockoff filter approach has similar performance to state-of-art Bayesian variable selection techniques, such as spike-and-slab priors, while outperforming classical variable selection methods, including classical knockoffs filter. Moreover, under more complex dependence structure of the covariates (as in Scenario 3), our proposal is able to control the FDR under any desired threshold, unlike spike-and-slab variable selection methods, that suffer from poor estimates of the PPIs. It also performs as well as classical knockoff filter with covariance structure known. This is relevant since in practice the precision matrix is never known.

Future work could extend this research in several directions. First, while we have assumed a standard Gaussian linear regression setting, similar Bayesian knockoff filters could be designed for linear settings that incorporate discrete-type responses. For example, in the simulations we have also considered an AFT model for survival outcomes. A similar extension, that uses data augmentation techniques, can be used for multinomial probit models



(Albert and Chib, 1993; Sha et al., 2004). Furthermore, logit and negative binomial responses could be accommodated via the use of Polya-Gamma data augmentation schemes (Polson et al., 2013; Zhou et al., 2012). Another interesting direction would be to extend the proposed knockoffs framework to the case of non-Gaussian covariates. The generation of knockoffs for non Gaussian random variables is still an open research problem. This case presents the main challenge of not having a known distribution that respects pairwise exchangeability (Bates et al., 2021). A promising direction is represented by the approach proposed by Dreassi et al. (2024), which makes use of conditional independence to build the knockoffs variables. Finally, the variable selection prior distribution we have used on the coefficients presents some computational challenges due to the need to use a Metropolis-within-Gibbs algorithm. Since the largest computational burden comes from the generation of the latent knockoffs at each MCMC iteration, a possible solution would be to use variational inference (Blei et al., 2017). However, the restrictive assumptions to obtain valid knockoffs require careful design of the approximate variational distributions. In particular, the commonly used mean field approximation cannot be used since it breaks the pairwise exchangeability assumption of the knockoffs and the covariates.

## References

- Albert, J. and Chib, S. (1993). Bayesian analysis of binary and polychotomous response data. *Journal of American Statistical Association*, 88:669–679.
- Barber, R. F. and Candès, E. (2015). Controlling the false discovery rate via knockoffs. *The Annals of Statistics*, 43(5):2055 – 2085.
- Barber, R. F. and Candès, E. (2019). A knockoff filter for high-dimensional selective inference. *The Annals of Statistics*, 47(5):2504–2537.
- Barber, R. F., Candès, E., and Samworth, R. J. (2020). Robust inference with knockoffs. *The Annals of Statistics*, 48(3):1409 – 1431.
- Barbieri, M. M. and Berger, J. O. (2004). Optimal predictive model selection. *The Annals of Statistics*, 32(3):870 – 897.

- Bates, S., Candès, E., Janson, L., and Wang, W. (2021). Metropolized knockoff sampling. *Journal of the American Statistical Association*, 116(535):1413–1427.
- Benjamini, Y. and Hochberg, Y. (1995). Controlling the false discovery rate: A practical and powerful approach to multiple testing. *Journal of the Royal Statistical Society: Series B (Methodological)*, 57(1):289–300.
- Benjamini, Y. and Yekutieli, D. (2001). The control of the false discovery rate in multiple testing under dependency. *The Annals of Statistics*, 29(4):1165–1188.
- Benjamini, Y. and Yekutieli, D. (2005). False discovery rate-adjusted multiple confidence intervals for selected parameters. *Journal of the American Statistical Association*, 100(469):71–81.
- Berti, P., Dreassi, E., Leisen, F., Pratelli, L., and Rigo, P. (2023). New perspectives on knockoffs construction. *Journal of Statistical Planning and Inference*, 223:1–14.
- Blei, D. M., Kucukelbir, A., and McAuliffe, J. D. (2017). Variational inference: A review for statisticians. *Journal of the American statistical Association*, 112(518):859–877.
- Brooks, S., Gelman, A., Jones, G., and Meng, X.-L. (2011). *Handbook of Markov Chain Monte Carlo*. CRC press.
- Brown, P. J., Vannucci, M., and Fearn, T. (1998). Multivariate bayesian variable selection and prediction. *Journal of the Royal Statistical Society: Series B (Statistical Methodology)*, 60(3):627–641.
- Candès, E., Fan, Y., Janson, L., and Lv, J. (2018). Panning for gold: ‘model-x’ knockoffs for high dimensional controlled variable selection. *Journal of the Royal Statistical Society: Series B (Statistical Methodology)*, 80(3):551–577.
- Carvalho, C. M., Polson, N. G., and Scott, J. G. (2010). The horseshoe estimator for sparse signals. *Biometrika*, 97(2):465–480.
- Castillo, I. and Roquain, É. (2020). On spike and slab empirical Bayes multiple testing. *The Annals of Statistics*, 48(5):2544–2574.

- Dai, C., Lin, B., Xing, X., and Liu, J. S. (2022). False discovery rate control via data splitting. *Journal of the American Statistical Association*, 118(544):2503–2520.
- Dreassi, E., Leisen, F., Pratelli, L., and Rigo, P. (2024). Generating knockoffs via conditional independence. *Electronic Journal of Statistics*, 18(1):119–144.
- Fan, J. and Li, R. (2001). Variable selection via nonconcave penalized likelihood and its oracle properties. *Journal of the American Statistical Association*, 96(456):1348–1360.
- Friedman, J., Hastie, T., and Tibshirani, R. (2008). Sparse inverse covariance estimation with the graphical LASSO. *Biostatistics*, 9(3):432–441.
- George, E. I. and McCulloch, R. E. (1997). Approaches for Bayesian variable selection. *Statistica Sinica*, 7(2):339–373.
- Geweke, J. (1992). Evaluating the accuracy of sampling-based approaches to the calculations of posterior moments. *Bayesian Statistics*, 4:641–649.
- Gu, J. and Yin, G. (2021). Bayesian knockoff filter using Gibbs sampler. *arXiv preprint arXiv:2102.05223*.
- Guindani, M., Müller, P., and Zhang, S. (2009). A Bayesian discovery procedure. *Journal of the Royal Statistical Society Series B: Statistical Methodology*, 71(5):905–925.
- Li, C. and Li, H. (2008). Network-constrained regularization and variable selection for analysis of genomic data. *Bioinformatics*, 24(9):1175–1182.
- Liu, H., Lafferty, J., and Wasserman, L. (2009). The Nonparanormal: Semiparametric estimation of high dimensional undirected graphs. *Journal of Machine Learning Research*, 10:2295–2328.
- Meinshausen, N. and Bühlmann, P. (2010). Stability selection. *Journal of the Royal Statistical Society: Series B (Statistical Methodology)*, 72(4):417–473.
- Meinshausen, N. and Bühlmann, P. (2006). High-dimensional graphs and variable selection with the lasso. *The Annals of Statistics*, 34(3):1436–1462.

- Mitchell, T. J. and Beauchamp, J. J. (1988). Bayesian variable selection in linear regression. *Journal of the American Statistical Association*, 83(404):1023–1032.
- Muller, P., Parmigiani, G., and Rice, K. (2006). FDR and Bayesian multiple comparisons rules. In *Proc. Valencia/ISBA 8th World Meeting on Bayesian Statistics, Benidorm (Alicante, Spain)*.
- Newton, M. A., Noueiry, A., Sarkar, D., and Ahlquist, P. (2004). Detecting differential gene expression with a semiparametric hierarchical mixture method. *Biostatistics*, 5(2):155–176.
- Park, T. and Casella, G. (2008). The Bayesian lasso. *Journal of the American Statistical Association*, 103(482):681–686.
- Peterson, C. B., Stingo, F. C., and Vannucci, M. (2016). Joint Bayesian variable and graph selection for regression models with network-structured predictors. *Statistics in Medicine*, 35(7):1017–1031.
- Polson, N. G., Scott, J. G., and Windle, J. (2013). Bayesian inference for logistic models using Pólya–Gamma latent variables. *Journal of the American Statistical Association*, 108(504):1339–1349.
- Ren, Z., Wei, Y., and Candès, E. (2023). Derandomizing knockoffs. *Journal of the American Statistical Association*, 118(542):948–958.
- Rothman, A. J., Bickel, P. J., Levina, E., and Zhu, J. (2008). Sparse permutation invariant covariance estimation. *Electronic Journal of Statistics*, 2(none):494 – 515. Publisher: Institute of Mathematical Statistics and Bernoulli Society.
- Savitsky, T., Vannucci, M., and Sha, N. (2011). Variable selection for nonparametric Gaussian process priors: Models and computational strategies. *Statistical Science*, 26(1):130–149.
- Scott, J. G. and Berger, J. O. (2010). Bayes and empirical-Bayes multiplicity adjustment in the variable-selection problem. *The Annals of Statistics*, 38(5):2587–2619.

- Sesia, M., Sabatti, C., and Candès, E. J. (2018). Gene hunting with hidden Markov model knockoffs. *Biometrika*, 106(1):1–18.
- Sha, N., Tadesse, M. G., and Vannucci, M. (2006). Bayesian variable selection for the analysis of microarray data with censored outcomes. *Bioinformatics*, 22(18):2262–2268.
- Sha, N., Vannucci, M., Tadesse, M. G., Brown, P. J., Dragoni, I., Davies, N., Roberts, T. C., Contestabile, A., Salmon, M., Buckley, C., et al. (2004). Bayesian variable selection in multinomial probit models to identify molecular signatures of disease stage. *Biometrics*, 60(3):812–819.
- Smith, A. F. (1973). A general Bayesian linear model. *Journal of the Royal Statistical Society: Series B (Methodological)*, 35(1):67–75.
- Stamey, T. A., Kabalin, J. N., McNeal, J. E., Johnstone, I. M., Freiha, F., Redwine, E. A., and Yang, N. (1989). Prostate specific antigen in the diagnosis and treatment of adenocarcinoma of the prostate. ii. radical prostatectomy treated patients. *The Journal of urology*, 141(5):1076–1083.
- Tadesse, M. G. and Vannucci, M., editors (2021). *Handbook of Bayesian Variable Selection*. Chapman and Hall/CRC.
- Tanner, M. A. and Wong, W. H. (1987). The calculation of posterior distributions by data augmentation. *Journal of the American Statistical Association*, 82(398):528–540.
- Tibshirani, R. (1996). Regression shrinkage and selection via the lasso. *Journal of the Royal Statistical Society Series B (Statistical Methodology)*, 58(1):267–288.
- Vannucci, M. (2021). Discrete spike-and-slab priors: Models and computational aspects. *Handbook of Bayesian Variable Selection*, pages 3–24.
- Villasenor Alva, J. A. and Estrada, E. G. (2009). A generalization of Shapiro–Wilk’s test for multivariate normality. *Communications in Statistics—Theory and Methods*, 38(11):1870–1883.

- Wang, H. (2015). Scaling It Up: Stochastic Search Structure Learning in Graphical Models. *Bayesian Analysis*, 10(2):351 – 377.
- Whittemore, A. S. (2007). A Bayesian false discovery rate for multiple testing. *Journal of Applied Statistics*, 34(1):1–9.
- Xing, X., Zhao, Z., and Liu, J. S. (2023). Controlling false discovery rate using Gaussian mirrors. *Journal of the American Statistical Association*, 118(541):222–241.
- Yap, J. K. and Gauran, I. I. M. (2023). Bayesian variable selection using knockoffs with applications to genomics. *Computational Statistics*, 38(4):1771–1790.
- Zhou, M., Li, L., Dunson, D., and Carin, L. (2012). Lognormal and gamma mixed negative binomial regression. In *Proceedings of the International Conference on Machine Learning. International Conference on Machine Learning*, pages 1343–1350. NIH Public Access.
- Zou, H. and Hastie, T. (2005). Regularization and variable selection via the elastic net. *Journal of the Royal Statistical Society: Series B (Statistical Methodology)*, 67(2):301–320.